

LATTICE
DYNAMICS

Studies of the Heat Capacity and Thermal Expansion of the $\text{Na}_{0.95}\text{K}_{0.05}\text{NbO}_3$ Solid Solution

M. V. Gorev^{a, b, *}, V. S. Bondarev^{a, b}, S. I. Raevskaya^c, M. P. Ivliev^c,
I. P. Raevskii^c, and I. N. Flerov^{a, b}

^a Kirensky Institute of Physics, Siberian Branch of the Russian Academy of Sciences,
Akademgorodok 50–38, Krasnoyarsk, 660036 Russia

* e-mail: gorev@iph.krasn.ru

^b Institute of Engineering Physics and Radio Electronics, Siberian Federal University,
ul. Kirenskogo 28, Krasnoyarsk, 660074 Russia

^c Research Institute of Physics, Southern Federal University, pr. Stachki 194, Rostov-on-Don, 344090 Russia

Received June 21, 2013

Abstract—The heat capacity and thermal expansion of ceramic samples of the $\text{Na}_{0.95}\text{K}_{0.05}\text{NbO}_3$ solid solution have been investigated over a wide temperature range of 100–750 K. The observed anomalies in the heat capacity and thermal expansion at $T_4 = 297$ K, $T_3 = 535$ K, $T_2 = 665$ K, and $T_1 \approx 710$ K correspond to the sequences of phase transitions $N \rightarrow Q \rightarrow G \rightarrow S \rightarrow T1$. It has been shown that, as a result of the phase transitions, the unit cell volume at T_4 and T_2 decreases, and at T_3 and T_1 , increases with increasing temperature. The directions of the shift of the phase transition temperatures induced by hydrostatic pressure have been determined. It has been established that all structural transformations are accompanied by relatively small variations in the entropy. Different mechanisms of the structural distortions have been discussed.

DOI: 10.1134/S1063783414020115

1. INTRODUCTION

Sodium niobate NaNbO_3 (NN) belonging to an extensive family of crystals with perovskite-type structure is characterized by a large number of structural phase transitions (PTs). Six dissymmetric phases have thus far been identified in NN [1]:

$$\begin{aligned} U(Pm\bar{3}m) &\leftrightarrow T2(P4/mbm) \leftrightarrow T1(Ccmm) \\ &\leftrightarrow S(Pmmn) \leftrightarrow R(Pmnm) \\ &\leftrightarrow P(Pbma) \leftrightarrow N(R3c). \end{aligned}$$

Considered from the viewpoint of crystallography, the totality of the observed structural transformations stems from the cubic lattice being unstable against distortions of two types, more specifically, displacements of anions of the oxygen sublattice, which may be interpreted as rotations of the octahedra (rotational distortions), and displacements of cations from centrosymmetric positions, which lead to the formation of ferroelectric and antiferroelectric states [2–5]. Three high-temperature PTs in NN derive from rotation of the octahedra, and three subsequent ones, from a combination of their rotations and “polarization,” which drive two antiferroelectric, intricately ordered phases (P and R) and a ferroelectric one (the low-temperature N). The whole set of the dissymmetric phases, with the exception of the P and R phases, can be described by three three-component order parameters, two of which, ψ and ϕ , relate to the rotations of

NbO_6 octahedra corresponding to the M_3 and R_{25} lattice vibrational modes, and one—to the p -uniform polarization driven by displacement of Nb cations from centers of the octahedra (Γ_{15} mode).

The diversity of the instabilities of the NN lattice accounts also for the complex polymorphism of NN-based solid solutions, in particular, of $\text{Na}_{1-x}\text{K}_x\text{NbO}_3$ (NKN), compounds enjoying wide application in piezoelectric technology. By mid-1970s, the structures of the phases observed in NKN have largely been studied, and the concentration T – x diagram of the phase states of this system was constructed [6, 7]. This was followed by reproduction of the main features of the phase diagram in terms of the Landau theory [8], although some of its essential aspects have not found explanation. A more detailed thermodynamic description of NKN and a refined T – x phase diagram built on its basis can be found in [9].

Although sodium niobate and the associated systems of solid solutions have been the subject of an extremely large number of studies, no truly comprehensive investigation of thermal characteristics in the region of the phase transitions and of the effect of thermal prehistory of a sample on the stability of the distorted phases has thus far been performed. Accumulation of the relevant information would provide a basis for formulation of more complete model ideas bearing on correlation among phenomena differing in physical nature. A large number of PTs observed in the NN and

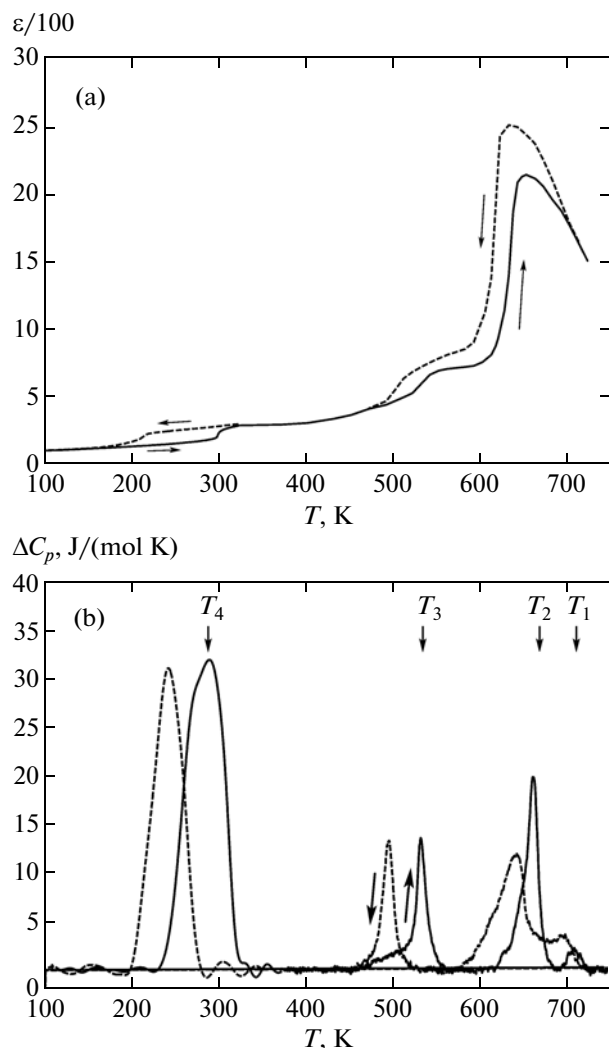


Fig. 1. Temperature dependences of (a) the permittivity and (b) the anomalous component of the heat capacity of the $\text{Na}_{0.95}\text{K}_{0.05}\text{NbO}_3$ ceramic sample measured during heating and cooling.

its solid solutions can be correlated with weak anomalies in the structural, electrophysical, and optical parameters, and data on the T - x diagrams based on the results obtained in such studies are fairly contradictory. Thermophysical methods are characterized by a high sensitivity and provide a possibility to detect any energy variations in a sample, irrespective of their nature; this means that they permit investigation of transitions driven both by ferroelastic and ferroelectric and antiferroelectric transformations.

We report here on studies of the permittivity, heat capacity, and thermal expansion of the $\text{Na}_{0.95}\text{K}_{0.05}\text{NbO}_3$ ceramics. The choice of this composition was motivated by the observation that its ferroelectric phase becomes stable already at room temperature, when several rotational phase transitions still

persist while disappearing already with potassium contents above 15 %.

2. EXPERIMENTAL TECHNIQUES AND RESULTS

2.1. Preparation of Samples and Dielectric Measurements

The $\text{Na}_{0.95}\text{K}_{0.05}\text{NbO}_3$ ceramic samples with a density of 92–95% of the theoretical value were prepared by standard technology (solid-phase synthesis from a mixture of Na_2CO_3 , K_2CO_3 , and Nb_2O_5 with subsequent calcination without pressure). The X-ray diffraction analysis demonstrated absence of non-perovskite phases. Dielectric permittivity measurements performed at a frequency of 100 kHz with a Wayne–Kerr 6500 impedance meter in the continuous cooling and heating mode with a rate of 2–3 K/min (Fig. 1a) revealed four features in the behavior of $\epsilon(T)$ related with phase transitions, whose temperatures ($T_4 \approx 300$ K, $T_3 \approx 530$ K, $T_2 \approx 660$ K, and $T_1 \approx 710$ K) in the heating mode correlate nicely with the T - x diagram of the (Na,K)NbO₃ system [9]. The temperature hysteresis of the transition to the low-temperature ferroelectric phase N , which in NN depends very strongly on sample defect structure [10, 11], is substantially larger than that in crystals with closer compositions [12].

2.2. Heat Capacity Studies

Comprehensive studies of the heat capacity in the 100–800 K temperature interval were performed with a differential scanning microcalorimeter (DSM-10Ma) in the dynamic mode with heating and cooling rates of 16 K/min in helium environment. The measurements were performed on ceramic samples ($m \sim 200$ mg) packed in an aluminum container. The scatter of experimental points from the smoothed curve did not exceed 1%. The error of determination of the integral characteristics (enthalpy and entropy) was within ~ 10 –15%.

Of most interest in an analysis of phase transitions is information on the anomalous heat capacity and entropy they are related to. Therefore, Fig. 1b shows a graph of the anomalous heat capacity component $\Delta C_p(T)$ obtained as a difference between the total and lattice heat capacity $C_p - C_L$. The latter was found by fitting the C_p data with a smooth polynomial function beyond the regions in which the heat capacity exhibits anomalous behavior. Four anomalies in the heat capacity were observed which become reproduced in different series of measurements in the form of peaks with maxima at the temperatures $T_4 = 295 \pm 5$ K, $T_3 = 532 \pm 2$ K, $T_2 = 660 \pm 5$ K, and $T_1 = 708 \pm 5$ K. The fairly large temperature hysteresis $\delta T_4 \approx 50$ K, $\delta T_3 \approx 36$ K, $\delta T_2 \approx 18$ K, and $\delta T_1 \approx 16$ K, as well as the practically symmetric shape of the ΔC_p peaks, suggest

strongly that all the PTs studied in NKN are clearly pronounced first-order transformations which are far away from the tricritical point.

2.3. Thermal Expansion

Thermal expansion was studied with a DIL-402C (NETZSCH) dilatometer in dynamic mode within the temperature variation interval 90–770 K at rates of 2–5 K/min. The measurements were run in helium flow. Calibration and monitoring of thermal expansion of the measurement system were performed with the use of fused silica standards.

Four successive series of measurements were conducted in identical conditions. Thermal cycling ensured reliable reproducibility of the results reflecting the behavior with temperature of the linear coefficient of thermal expansion $\alpha(T)$. Because the measurements were performed on a ceramic sample, information on the volume thermal expansion coefficient was obtained under the assumption that $\beta(T) = 3\alpha(T)$. In all the cases studied, four clearly pronounced anomalies in $\beta(T)$ were detected at temperatures $T_4 = 299 \pm 1$ K, $T_3 = 537 \pm 1$ K, $T_2 = 670 \pm 1$ K, and $T_1 \approx 710$ K (Fig. 2), in satisfactory agreement with the data amassed in calorimetric and dielectric measurements.

Only the results obtained in the first series of measurements deviate somewhat from the overall pattern in slightly smaller anomalies in β at 299, 537, and 670 K. The phase transition temperatures vary from one measurement series to another within ± 1 K. Such a behavior of thermal expansion can be assigned both to defect and stress annealing brought about in the first heating up to 770 K and to variations in composition (stoichiometry) initiated in the sample exposed to helium, i.e., oxygen-free environment at high temperatures.

The measurements performed in the heating and cooling modes have permitted determination of the temperature hysteresis of the first-order PT: $\delta T_3 = 34$ K, $\delta T_2 = 15$ K, and $\delta T_1 = 10$ K. Regrettably, because of the specific design of the dilatometer employed measurements in the cooling mode in the region of the PT at 300 K could not be performed, so that the δT_4 hysteresis was left unmeasured. Note the satisfactory agreement between the values of T_i and δT_i found in dielectric, calorimetric and dilatometric measurements which were performed at noticeably different rates of temperature variation. The large values of δT_i are likewise a testimony to the first-order PTs studied being far from the tricritical point.

3. DISCUSSION

3.1. Interpretation of the Anomalies

A comparison of the results obtained with the data amassed in studies of the structure and ferroelectric properties, as well as with concentration phase dia-

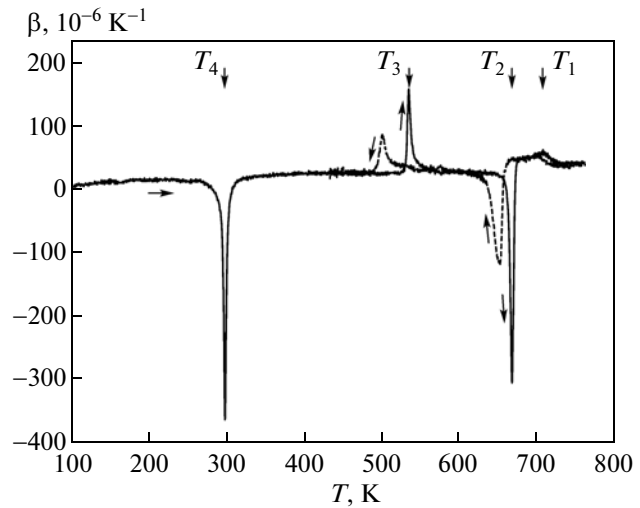
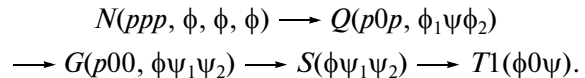


Fig. 2. Temperature dependences of the volume thermal expansion coefficient $\beta(T)$ of $\text{Na}_{0.95}\text{K}_{0.05}\text{NbO}_3$ measured during heating and cooling.

grams [6–9, 13] strongly suggests that the observed anomalies in the permittivity, heat capacity and thermal expansion of the $\text{Na}_{0.95}\text{K}_{0.05}\text{NbO}_3$ solid solution are related to the phase transition sequence



We have not detected any reproducible anomalous behavior of the heat capacity and thermal expansion in the 420–500 K temperature interval, where in NN and (Na,K)NbO₃ crystals with a small content of potassium anomalies in the dielectric properties, lattice parameters and Raman spectra were observed [12, 14, 15], which the authors associated with formation of an incommensurate phase. Neither did we observe anomalous behavior in $C_p(T)$ and $\beta(T)$ in the 600–650 K interval, in which a transition between the G and F phases is assumed [12] to occur. The latter point suggests strongly that in the $T-x$ phase diagram the concentration of potassium in the solid solution studied by us is less than would be required for the $G-F-T1$ triple point (Fig. 3).

3.2. Analysis of the Entropy

Distortions of the crystal lattice caused by structural PTs are considered fairly frequently as associated with one of the two limiting mechanisms, namely, of the displacement or order–disorder types. Features inherent in both mechanisms can become manifest in some form, as a rule, in the behavior of different physical properties of the same crystal. Thus one of the key points consists in identifying the mechanism playing the dominant part in each particular case.

The PT-type displacement in oxygen crystals with perovskite structure is argued for by some experimen-

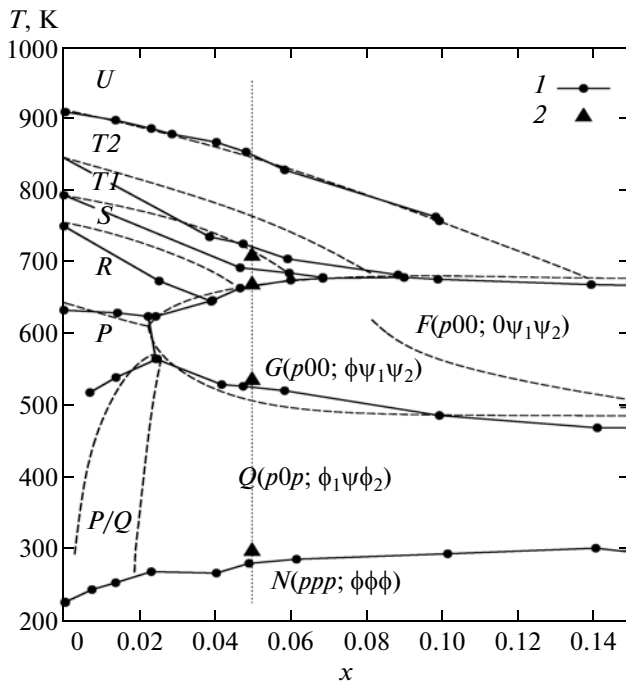


Fig. 3. Concentration phase diagram of the $\text{Na}_{1-x}\text{K}_x\text{NbO}_3$ system: (1) results of dielectric measurements [9] and (2) data from the present study. Dashed lines represent the data taken from [6, 7].

tal evidence. In these compounds one observed soft modes in the starting and the distorted phases, large values of the Curie constants and, as a rule, small variations of the entropy. Also, comprehensive microscopic calculations [16–18] did not evidence any grounds for evolvment in the cubic phase of ABO_3 ferroelectric perovskites of any factor that could generate centers of equilibrium driven by a static displacement of ion B in a unit cell other than the center of the cube formed by ions A .

At the same time some experimental observations were interpreted as proofs for existence of local structural distortions above the PT temperature, more specifically, diffuse X-ray scattering, the central peak in light scattering, birefringence and excessive heat capacity. These results spurred development of various theoretical models identifying phase transitions in perovskites with order–disorder-type transformations.

To cite an example, analysis of EXAFS spectra of the cubic phases of NaNbO_3 and KNbO_3 culminated in a suggestion [13, 19] that the graphs of potential energy of the Nb cation in both compounds are similar and have eight minima that can be associated with its displacement from the center of the oxygen octahedron along the [111] directions by 0.16 and 0.19 Å, accordingly. These observations led to the conclusion that the instability in the appearance of polarization in the niobates can be assigned to the Nb cations tending

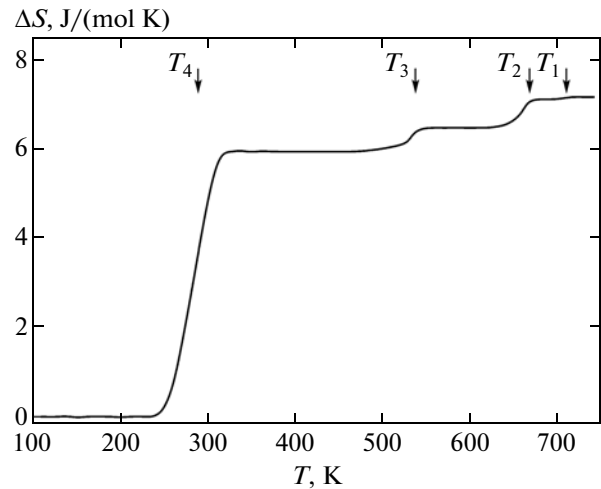


Fig. 4. Temperature dependence of the anomalous component of the entropy of $\text{Na}_{0.95}\text{K}_{0.05}\text{NbO}_3$.

to become ordered accordingly, and the phase transitions driven by this instability, to transitions of the order–disorder type.

The pattern of ferroelectric ordering in $\text{Na}_{1-x}\text{K}_x\text{NbO}_3$ solid solutions [9, 12] with small x , disregarding the presence of rotational distortions, correlates with that of pure KNbO_3 (KN); indeed, cooling induces first condensation of one polarization component ($p_1 \neq 0, p_2 = p_3 = 0$) in the G or F phases, next of two of them ($p_1 = p_2 \neq 0, p_3 = 0$) in the Q phase, and, further, of three components ($p_1 = p_2 = p_3 \neq 0$) in the N phase, combinations which in the ordering model should bring about entropy variations $R \ln 2$, where R is the universal gas constant, in each of the consecutive PTs.

The variation of the entropy in $\text{Na}_{0.95}\text{K}_{0.05}\text{NbO}_3$ obtained from calorimetric data and derived by integrating the $\Delta C_p(T)/T$ function is presented graphically in Fig. 4. The total entropy variation ΔS associated with the PT sequence $N \rightarrow Q \rightarrow G \rightarrow S \rightarrow T_1$ adds up to 7.2 J/(mol K). Separating the anomalous components of entropy for each of the PTs meets with difficulties, because the anomalies in heat capacity are diffuse and overlap. Only an estimate of ΔS_i appears possible: $\Delta S_4 \approx 5.9$ J/(mol K), $\Delta S_3 \approx 0.55$ J/(mol K), $\Delta S_2 \approx 0.6$ J/(mol K), and $\Delta S_1 \approx 0.1$ J/(mol K). The values of ΔS thus obtained correlate with the data presented in [20] while exceeding slightly those of [21]. The entropy variations in NaNbO_3 ($\Sigma \Delta S_i = 4.0$ J/(mol K) [22]) and in KNbO_3 ($\Sigma \Delta S_i = 2.4$ J/(mol K) [23]), which reveals no rotational distortions altogether, are still smaller.

According to traditional concepts, such variations of entropy permit assigning the above PTs to displacement-type transformations. However, as shown in [24, 25], a small value of the entropy variation cannot in itself be considered as an unambiguous indication that

a PT is a displacement-type transition. As pointed out in the above papers, BaTiO_3 , KNbO_3 , NaNbO_3 , and a number of other compounds are specific in that even in the symmetric, cubic phase they have coupled chains consisting of ten and more unit cells. At a PT these chains become ordering as a whole. Accordingly, entropy variation per particle will be much smaller than $R\ln 2$. This is why order–disorder-type PTs in such compounds may be accompanied by comparatively small variations of entropy.

Recent years have given birth to a viewpoint applicable at least to perovskites, by which neither models of the order–disorder-type transitions nor the scenario involving a soft mode separately, i.e., in a “pure form,” cannot be used alone to describe a ferroelectric PT [26, 27]. Actually, PTs into ferroelectric phases involve a peculiar “hybridization” of crystal softening processes over one of the lattice vibration modes and particle redistribution over crystallographically equivalent positions.

The above analysis strongly suggests that genesis of phase states in the compound under consideration follows an extremely complex pattern, thus making a straightforward, unique interpretation of the results obtained does not appear possible at this time.

3.3. Effect of Pressure on the Arrangement of Phase Boundaries

Introduction into KNbO_3 of the Na^+ ion with the ionic radius substantially smaller than that of K^+ is equivalent to application of hydrostatic “chemical” pressure. As hydrostatic pressure increases, the region of thermodynamic stability of phases with a smaller unit cell volume should expand in the T – p diagram at the expense of phases with a larger unit cell volume. This implies that the region occupied by the Q phase should broaden at the expense of phases G and N , and of the S phase, at the expense of phases G and T_1 . On the other hand, growth of hydrostatic pressure brings about a decrease of the unit cell volume. In the concentration diagram this translates into a decrease of potassium concentration. Indeed, as the concentration of K decreases, the PT points in the diagram between phases N and Q , S and G shift down in temperature, and those between phases Q and G , S and T_1 , up, i.e., we observe exactly the pattern assumed to form.

As already mentioned, PTs in $\text{Na}_{0.95}\text{K}_{0.05}\text{NbO}_3$ represent essentially clearly pronounced first-order transformations, so that the variations of entropy determined in our experiments may be considered as jumps of entropy at the phase transition point. This offers us a possibility of estimating the effect of hydrostatic

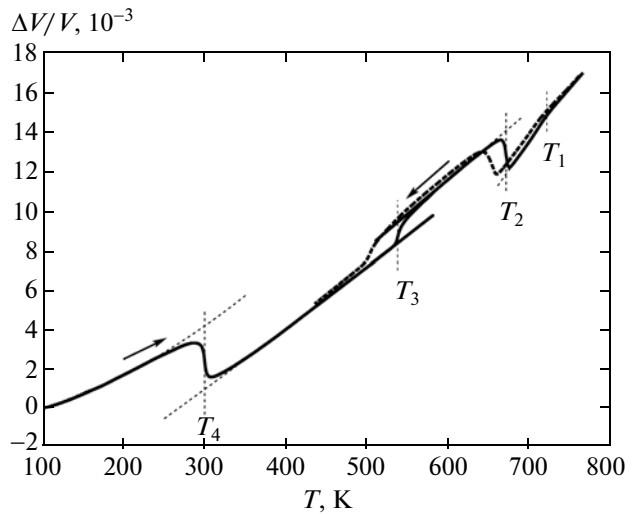


Fig. 5. Temperature dependences of the volume deformation $\Delta V/V$ of $\text{Na}_{0.95}\text{K}_{0.05}\text{NbO}_3$ measured during heating and cooling.

pressure on the temperatures of first-order PTs from the Clapeyron–Clausius relation

$$\frac{dT_0}{dp} = \frac{\delta V}{\delta S} = V_m \frac{\delta V/V}{\delta S},$$

where V_m is the molar volume, $\delta V/V$ and δS are the jumps the volume deformation and entropy experience at a phase transition.

The temperature dependences of the volume deformation $\Delta V/V$ measured in the heating and cooling modes are presented graphically in Fig. 5.

As the temperature increases, the volume decreases in the N – Q ($\delta V/V \approx -3.2 \times 10^{-3}$) and G – S ($\delta V/V \approx -2.2 \times 10^{-3}$) PTs, and increases in the Q – G PT ($\delta V/V \approx 1.1 \times 10^{-3}$). The temperature dependences of deformation outside the regions of anomalous behavior were described by first- or second-order polynomials, and the jumps $\delta V/V$, derived by extrapolating the polynomials to the temperatures of first-order phase transitions (Fig. 5).

Our estimation yielded the following baric coefficients: $(dT/dp)_1 > 0$, $(dT/dp)_2 \approx -80$ K/GPa, $(dT/dp)_3 \approx 73$ K/GPa, and $(dT/dp)_4 \approx -20$ K/GPa.

It should be stressed that a decrease of the cubic lattice constant affects only weakly in itself the degree of instability with respect to the appearance of polarization. The Curie–Weiss temperatures for KNbO_3 , NaNbO_3 and AgNbO_3 extrapolated from the cubic phase were shown [13] to be practically equal. The appearance of rotational distortions produces a much more pronounced effect. Indeed, rotation of octahedra about all the three axes results in a noticeable decrease of the temperature of the PT from the paraelectric phase S into the ferroelectric phase G in

the $0.04 < x < 0.06$ interval (Fig. 3) [9]. Recalling that hydrostatic pressure induces rotational distortions suppressing the ferroelectric transition, it becomes clear why the temperature of the $S-G$ transition decreases. One of the factors accounting for the $Q-G$ PT temperature increase may be that the instability of phase G with respect to appearance of the second order-parameter component which relates to polarization is induced to a certain extent by rotational distortions. As for the $N-Q$ PT, this situation appears here fairly complex requiring a more comprehensive investigation. It is known, for instance, that in NaNbO_3 crystals with oxygen nonstoichiometry which contain large inclusions of the Q phase the transition evolves not directly into the N phase but rather in the $Q-P-N$ sequence under cooling, and the $N-P-Q$ one under heating [11]. Dielectric measurements suggested earlier a similar phase transition sequence also in NKN crystals with a low K content [12].

4. CONCLUSIONS

The dielectric, calorimetric, and dilatometric studies of the $\text{Na}_{0.95}\text{K}_{0.05}\text{NbO}_3$ ceramic sample revealed anomalies in the behavior of permittivity, heat capacity, and thermal expansion associated with consecutive phase transitions in the sequence $T1-S-G-Q-N$. It has been shown that hydrostatic “chemical” pressure inducing rotational distortions is one of the most essential factors governing variations in the arrangement of phase boundaries.

ACKNOWLEDGMENTS

This study was supported by the Council on Grants from the President of the Russian Federation for Support of Leading Scientific Schools of the Russian Federation (grant no. NSh-4828.2012.2) and the Russian Foundation for Basic Research (project no. 12-02-31799 mol_a).

REFERENCES

1. H. Megaw, *Ferroelectrics* **7**, 87 (1974).
2. L. E. Cross and B. J. Nicholson, *Philos. Mag.* **46** (376), 453 (1955).
3. R. Ishida and G. Honjo, *J. Phys. Jpn.* **34**, 1279 (1973).
4. K. S. Aleksandrov, A. T. Anistratov, B. V. Beznosikov, and N. V. Fedoseeva, *Phase Transitions in ABX₃ Halide Crystals* (Nauka, Novosibirsk, 1981) [in Russian].
5. G. A. Smolenskii, V. A. Bokov, V. A. Isupov, N. N. Krainik, R. E. Pasyukov, A. I. Sokolov, and N. K. Yushin, *Physics of Ferroelectric Phenomena* (Nauka, Leningrad, 1985) [in Russian].
6. M. Ahtee and A. M. Glazer, *Acta Crystallogr., Sect. A: Cryst. Phys., Diffr., Theor. Gen. Crystallogr.* **32**, 434 (1976).

7. M. Ahtee and A. W. Hewat, *Acta Crystallogr., Sect. A: Cryst. Phys., Diffr., Theor. Gen. Crystallogr.* **34**, 309 (1978).
8. C. N. W. Darlington, *Philos. Mag.* **31**, 1159 (1975).
9. M. P. Ivliev, I. P. Raevskii, L. A. Reznichenko, S. I. Raevskaya, and V. P. Sakhnenko, *Phys. Solid State* **45** (10), 1984 (2003).
10. S. I. Raevskaya, I. P. Raevskii, S. P. Kubrin, M. S. Panchelyuga, V. G. Smotrakov, V. V. Eremkin, and S. A. Prosandeev, *J. Phys.: Condens. Matter* **20**, 232202 (2008).
11. R. A. Shakhovoy, S. I. Raevskaya, L. A. Shakhovaya, D. V. Suzdalev, I. P. Raevskii, Yu. I. Yuzyuk, A. F. Semchench, and M. El Marssi, *J. Raman Spectrosc.* **43**, 1141 (2012).
12. I. P. Raevskii, L. A. Reznichenko, M. P. Ivliev, V. G. Smotrakov, V. V. Eremkin, M. A. Malitskaya, L. A. Shilkina, S. I. Shevtsova, and A. V. Borodin, *Crystallogr. Rep.* **48** (3), 486 (2003).
13. M. P. Ivliev, S. I. Raevskaya, I. P. Raevskii, V. A. Shuvaeva, and I. P. Pirog, *Phys. Solid State* **49** (4), 769 (2007).
14. L. A. Reznichenko, L. A. Shilkina, E. S. Gagarina, I. P. Raevskii, E. A. Dul'kin, E. M. Kuznetsova, and V. V. Akhnazarova, *Crystallogr. Rep.* **48** (3), 448 (2003).
15. I. P. Raevskii, M. P. Ivliev, L. A. Reznichenko, M. N. Palatnikov, L. E. Balyunis, and M. A. Malitskaya, *Tech. Phys.* **47** (6), 772 (2002).
16. O. E. Kvyatkovskii, *Phys. Solid State* **43** (8), 1401 (2001).
17. B. D. Chapman, E. A. Stern, S.-W. Han, J. O. Cross, G. T. Seidler, V. Gavril'yatchenko, R. V. Vedrinskii, and V. L. Kraizman, *Phys. Rev. B: Condens. Matter* **71**, 020102(R) (2005).
18. E. G. Maksimov and N. L. Matsko, *J. Exp. Theor. Phys.* **108** (3), 435 (2009).
19. M. P. Lemeshko, E. S. Nazarenko, A. A. Gonchar, L. A. Reznichenko, N. I. Nedoseykina, A. A. Novakovich, O. Mathon, Y. Joly, and R. V. Vedrinskii, *Phys. Rev. B: Condens. Matter* **76**, 134106 (2007).
20. V. J. Tennery and K. W. Hang, *J. Appl. Phys.* **39**, 4749 (1968).
21. G. Shirane, R. Newnham, and R. Pepinsky, *Phys. Rev.* **96**, 581 (1954).
22. V. S. Bondarev, A. V. Kartashev, M. V. Gorev, I. N. Fleurov, E. I. Pogorel'tsev, M. S. Molokeev, S. I. Raevskaya, D. V. Suzdalev, and I. P. Raevskii, *Phys. Solid State* **55** (4), 821 (2013).
23. G. Shirane, H. Donner, A. Pavlovic, and R. Pepinsky, *Phys. Rev.* **93**, 672 (1954).
24. M. Lambert and R. Comes, *Solid State Commun.* **7**, 305 (1969).
25. R. Comes, M. Lambert, and A. Guinier, *Acta Crystallogr., Sect. A: Cryst. Phys., Diffr., Theor. Gen. Crystallogr.* **26**, 244 (1970).
26. R. Pirc and R. Blinc, *Phys. Rev. B: Condens. Matter* **70**, 134107 (2004).
27. Y. G. Girshberg and Y. Yacoby, *J. Phys.: Condens. Matter* **11**, 9807 (1999).

Translated by G. Skrebtsov